

Accelerating Coupled Circuit-EM Simulation in the Frequency and Time Domain

Vikram Jandhyala, Swagato Chakraborty, Dipanjan Gope, and Chuanyi Yang

Applied Computational Electromagnetics Lab

Department of Electrical Engineering

University of Washington

Seattle, USA

jandhyala@ee.washington.edu

Abstract—An accelerated, full-wave, coupled electromagnetic-circuit simulation methodology is described. The simulator enables rapid modeling of high-speed effects in mixed-signal and RF circuits, and captures effects in both frequency and time domains.

Keywords- *method of moments, boundary element methods, coupled simulation, high-speed circuits, mixed-signal simulation*

I INTRODUCTION

Emerging applications in mixed-signal, RF, and analog micro-systems necessitate high-speed and high-frequency operation. As a result, coupling effects including crosstalk, substrate noise, dielectric loss, and radiation are dominant and need to be accounted for in the design stage. This is best done through integrated field solvers that either couple directly to circuit solvers or produce behavioral models that can be used in circuit simulation.

3D electromagnetic (EM) field solvers rely on standard approaches including the finite difference time domain, finite element, or method of moment (MoM) techniques. Over the past few years, MoM-based approaches have proven to be particularly useful for the simulation of all relevant EM effects in high-speed microelectronic subsystems. In conjunction with the rapidly maturing field of reduced computational complexity fast solvers, these are proving to be competitive or superior to partial differential equation based techniques for a wide class of problems encountered in microelectronics, although ultimately a hybrid approach for generalized solution may become the eventual standard. This paper summarizes and discusses advances in MoM methods related to this application area; in particular, coupled simulation of distributed electromagnetics effects and lumped circuit models, fast solvers, and extensions to existing time domain simulation schemes [1] are discussed.

The rest of the paper is organized as follows. The circuit-EM formulation is described in terms of integral equations. The acceleration of the coupled matrix is described next, followed by simulation results.

II COUPLED FORMULATION

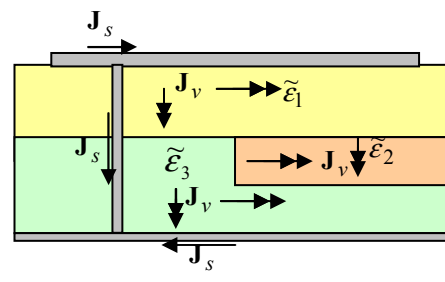


Figure 1. Equivalent surface current and volumetric polarization current in the hybrid model. Single arrows depict equivalent surface current and double arrows show volume polarization current.

A microelectronic sub-system consists of metallic structures such as interconnects, on-chip inductors, vias, power-ground planes, and also finite layers of lossy dielectric material as in Fig. 1. In the presented formulation MoM is used to model the electromagnetic interactions between the conducting and dielectric objects. The dielectric object is replaced by volumetric polarization currents radiating in the background medium and the conducting object is modeled with equivalent surface currents, also radiating in the background medium. The volumetric formulation for dielectric bodies allows convenient modeling of inhomogeneous multilayered finite dielectric regions, whereas the surface formulation obviates the need for explicit skin-depth based discretization of the conducting object, thus reducing the number of unknowns and also avoiding frequency dependent meshing of the conducting objects.

The formulation proceeds as follows. Firstly, the tangential electric field on a conducting surface vanishes, resulting in the equation

$$\left(\mathbf{E}_s^{scat}(\mathbf{J}_s) + \mathbf{E}_s^{scat}(\mathbf{J}_v) + Z_s \mathbf{J}_s + \mathbf{E}_s^{exc} \right)_{tan} = 0 \quad (1)$$

where $\mathbf{E}_s^{scat}(\mathbf{J}_s)$ and $\mathbf{E}_s^{scat}(\mathbf{J}_v)$ are the scattered electric field on the surface of the conductor due to the surface current \mathbf{J}_s and the volumetric current \mathbf{J}_v respectively. Z_s is the surface impedance given by $Z_s(\omega) = (1+j)\sqrt{\omega\mu/2\sigma}$ in

frequency domain and $Z_s(t) = \sqrt{\mu / \pi \sigma t}$ in time domain, μ is the background permeability, ω is the angular frequency and σ is the metal conductivity. E^{exc} is the electric field excitation caused by a delta gap source or incident electric field. Such an approach, coupled to circuit simulation enables modeling of conducting sections in a microelectronic circuit [2]. To include dielectric material effects, the relation between the electric flux density and the polarization current [3] provides the volumetric equation

$$\tilde{\epsilon}_v (\mathbf{E}_v^{scat}(\mathbf{J}_s) + \mathbf{E}_v^{scat}(\mathbf{J}_v) + \mathbf{E}_v^{exc}) = \frac{\mathbf{J}_v \tilde{\epsilon}_v}{(\tilde{\epsilon}_v - \tilde{\epsilon}_b)} \quad (2)$$

$\tilde{\epsilon}_b$ represents the dielectric constant of the background, and $\tilde{\epsilon}_v$ is the dielectric constant of the a lossy dielectric region. The contribution of the current to the scattered electric field is computed as a convolution of the source current and the background medium Green's function. The Green's function in the frequency domain is given by $G(\mathbf{r}, \mathbf{r}') = e^{j\tilde{k}_b |\mathbf{r} - \mathbf{r}'|} / (4\pi |\mathbf{r} - \mathbf{r}'|)$, \tilde{k}_b is the wave number in the background medium which can in general be complex for a frequency domain method. In the time domain the decaying wake in the Green's function for a lossy background medium is modeled through a recursive summation of decaying exponentials.

For microelectronic applications, it often suffices to model certain portions of the geometry with lumped circuit elements rather than a distributed EM model. For example a collection of a large number of vias can be replaced with an equivalent circuit comprising of resistances, and self and mutual inductances. Such an approximation is still sufficient in several cases for the desired level of model accuracy, and may provide massive savings in the computation cost and memory compared to a flat, brute-force approach. The proposed coupled EM-circuit technique provides a methodology [2] for such a hierarchical model.

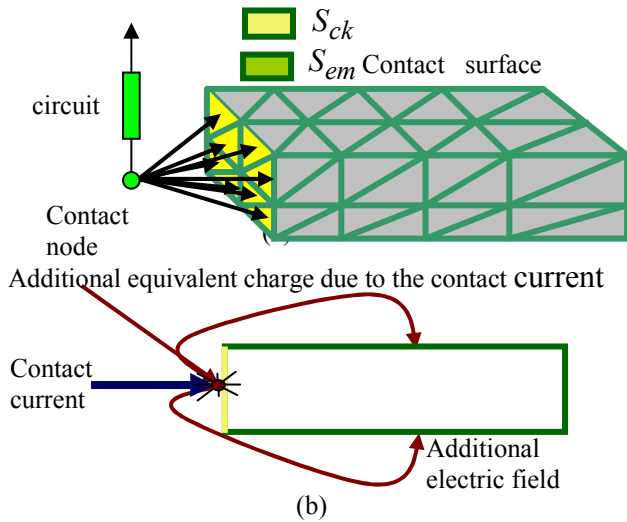


Figure 2. F (a) Classification of surface and (b) effect of the contact current

This work was partially supported by DARPA-MTO NeoCAD grant N66001-01-1-8920, NSF-CAREER grant ECS-0093102, NSF-SRC Mixed-Signal Initiative grant CCR-0120371)

The circuit and the electromagnetic domains are connected through a section of the conducting surface called the contact surface (Fig. 2a). On the contact surface the current continuity equation is modified as,

$$\begin{aligned} \nabla \cdot \mathbf{J}_s(\mathbf{r}') + j\omega \rho_s(\mathbf{r}') &= I / A, & \mathbf{r}' \in S_{ck} \\ \nabla \cdot \mathbf{J}_s(\mathbf{r}') + \frac{\partial}{\partial t} \rho_s(\mathbf{r}') &= I / A, & \mathbf{r}' \in S_{ck} \end{aligned} \quad (3)$$

for the frequency and time domains, respectively. ρ_s is the equivalent surface charge density, I is the contact current flowing into the contact surface from the circuit, and A is the contact area. The additional term in the right-hand side of (3) acts as an equivalent surface charge source (Fig. 2b) and generates an electric field. In terms of the system matrix, this introduces an additional set of unknowns namely the strengths of the coupling currents. In order to balance these extra unknowns a set of new equations is added that equates the potential of the contact surface to that of the corresponding circuit nodes. The final coupled EM-circuit system matrix has the following structure:

$$\begin{bmatrix} \overline{\overline{\mathbf{Z}}}_{EM} & \overline{\overline{\mathbf{Z}}}_{C2EM} & \overline{\mathbf{0}} \\ \overline{\overline{\mathbf{Z}}}_{EM2C} & \overline{\overline{\mathbf{Z}}}_{C2C} & \overline{\overline{\mathbf{C}}}_1 \\ \overline{\mathbf{0}} & \overline{\overline{\mathbf{C}}}_2 & \overline{\overline{\mathbf{Z}}}_{MNA} \end{bmatrix} \begin{bmatrix} \overline{\mathbf{X}}_{EM} \\ \overline{\mathbf{X}}_{Con.} \\ \overline{\mathbf{X}}_{MNA} \end{bmatrix} = \begin{bmatrix} \overline{\mathbf{R}}_{EM} \\ \overline{\mathbf{0}} \\ \overline{\mathbf{R}}_{MNA} \end{bmatrix} \quad (4)$$

$$\begin{bmatrix} \overline{\overline{\mathbf{Z}}}_{EM}^0 & \overline{\overline{\mathbf{Z}}}_{C2EM}^0 & \overline{\mathbf{0}} \\ \overline{\overline{\mathbf{Z}}}_{EM2C}^0 & \overline{\overline{\mathbf{Z}}}_{C2C}^0 & \overline{\overline{\mathbf{C}}}_1 \\ \overline{\mathbf{0}} & \overline{\overline{\mathbf{C}}}_2 & \overline{\overline{\mathbf{Z}}}_{MNA}^0 \end{bmatrix} \begin{bmatrix} \overline{\mathbf{X}}_{EM}(t_l) \\ \overline{\mathbf{X}}_{Con.}(t_l) \\ \overline{\mathbf{X}}_{MNA}(t_l) \end{bmatrix} = \begin{bmatrix} \overline{\mathbf{R}}_{EM}(t_l) \\ \overline{\mathbf{0}} \\ \overline{\mathbf{R}}_{MNA}(t_l) \end{bmatrix} + \sum_{k=1}^l \begin{bmatrix} \overline{\overline{\mathbf{Z}}}_{EM}^k & \overline{\overline{\mathbf{Z}}}_{C2EM}^k & \overline{\mathbf{0}} \\ \overline{\overline{\mathbf{Z}}}_{EM2C}^k & \overline{\overline{\mathbf{Z}}}_{C2C}^k & \overline{\overline{\mathbf{C}}}_1 \\ \overline{\mathbf{0}} & \overline{\overline{\mathbf{C}}}_2 & \overline{\overline{\mathbf{Z}}}_{MNA}^k \end{bmatrix} \begin{bmatrix} \overline{\mathbf{X}}_{EM}(t_{l-k}) \\ \overline{\mathbf{X}}_{Con.}(t_{l-k}) \\ \overline{\mathbf{X}}_{MNA}(t_{l-k}) \end{bmatrix} \quad (5)$$

in the frequency and time domains, respectively, where $\overline{\overline{\mathbf{Z}}}_{EM}$ is the electric field due to the surface and volume currents, $\overline{\overline{\mathbf{Z}}}_{C2EM}$ represents the contribution of the contact currents to the electric field, $\overline{\overline{\mathbf{Z}}}_{EM2C}$, represents the effect of the surface and volumetric currents on the contact potential, and $\overline{\overline{\mathbf{Z}}}_{C2C}$ represents the effect of the contact currents on the contact potential. The two zero blocks imply that there is no direct interaction between the EM and the circuit domain, except through the contact variables. $\overline{\overline{\mathbf{C}}}_1$ and $\overline{\overline{\mathbf{C}}}_2$ are connectivity matrices between the circuit and the contact quantities, and are transposes of each other. $\overline{\overline{\mathbf{Z}}}_{MNA}$ is the standard modified nodal analysis matrix for the lumped circuit

sections. On the right-hand side $\bar{\mathbf{R}}_{EM}$ is the tested exciting field, if any, and $\bar{\mathbf{R}}_{MNA}$ comprises of independent voltage and current sources. The superscript in the time domain version indicates the time step.

The coupled system in (4,5) can be solved using direct or accelerated iterative techniques to obtain the equivalent surface and volumetric currents as well as the node voltages and branch currents associated with the lumped circuit portion. Alternatively it is also possible to obtain an equivalent terminal representation for the structure modeled with distributed effects. This representation can be directly used as a stamp in the MNA. In the frequency domain the terminal model is obtained as an admittance matrix given by

$$\bar{\bar{\mathbf{T}}} = -\begin{bmatrix} \bar{\mathbf{0}} & \bar{\mathbf{C}}_2 \end{bmatrix} \begin{bmatrix} \bar{\mathbf{Z}}_{EM} & \bar{\mathbf{Z}}_{C2EM} \\ \bar{\mathbf{Z}}_{EM2C} & \bar{\mathbf{Z}}_{C2C} \end{bmatrix}^{-1} \begin{bmatrix} \bar{\mathbf{0}} \\ \bar{\mathbf{C}}_1 \end{bmatrix} \quad (6a)$$

and an excitation term given by

$$\bar{\mathbf{R}} = -\begin{bmatrix} \bar{\mathbf{0}} & \bar{\mathbf{C}}_2 \end{bmatrix} \begin{bmatrix} \bar{\mathbf{Z}}_{EM} & \bar{\mathbf{Z}}_{C2EM} \\ \bar{\mathbf{Z}}_{EM2C} & \bar{\mathbf{Z}}_{C2C} \end{bmatrix}^{-1} \begin{bmatrix} \bar{\mathbf{R}}_{EM} \\ \bar{\mathbf{0}} \end{bmatrix} \quad (6b)$$

Similarly for time domain we obtain an equivalent matrix stamp given by

$$\bar{\bar{\mathbf{T}}} = -\begin{bmatrix} \bar{\mathbf{0}} & \bar{\mathbf{C}}_2 \end{bmatrix} \begin{bmatrix} \bar{\mathbf{Z}}_{EM}^0 & \bar{\mathbf{Z}}_{C2EM}^0 \\ \bar{\mathbf{Z}}_{EM2C}^0 & \bar{\mathbf{Z}}_{C2C}^0 \end{bmatrix}^{-1} \begin{bmatrix} \bar{\mathbf{0}} \\ \bar{\mathbf{C}}_1 \end{bmatrix} \quad (7a)$$

and an excitation term as

$$\bar{\mathbf{R}}(t_j) = -\begin{bmatrix} \bar{\mathbf{0}} & \bar{\mathbf{C}}_2 \end{bmatrix} \begin{bmatrix} \bar{\mathbf{Z}}_{EM}^0 & \bar{\mathbf{Z}}_{C2EM}^0 \\ \bar{\mathbf{Z}}_{EM2C}^0 & \bar{\mathbf{Z}}_{C2C}^0 \end{bmatrix}^{-1} \sum_{i=1}^j \begin{bmatrix} \bar{\mathbf{Z}}_{EM}^i & \bar{\mathbf{Z}}_{C2EM}^i \\ \bar{\mathbf{Z}}_{EM2C}^i & \bar{\mathbf{Z}}_{C2C}^i \end{bmatrix} \begin{bmatrix} \bar{\mathbf{X}}_{EM}(t_{j-i}) \\ \bar{\mathbf{X}}_{Con.}(t_{j-i}) \end{bmatrix} + \begin{bmatrix} \bar{\mathbf{R}}_{EM}(t_j) \\ \bar{\mathbf{0}} \end{bmatrix} \quad (7b)$$

The stamp corresponding to the distributed model of a certain microelectronic structure can be stored in a library and can be coupled to any lumped elements for future analysis. It should be noted that for a structure with significant time delays, the time domain stamp will require an enhanced version of SPICE that can accommodate a time history of multiple time steps.

III ACCELERATION OF COUPLED SOLUTION

In the presented work, QR compression on a pre-determined interaction list reduces the setup-time as compared to binary tree-based methods without compromising on the memory or solve-time and thereby yields an overall high efficiency solver. This section describes this method, termed the PILOT algorithm and its application to full-wave modeling of circuit problems [4]. The novel features in the presented algorithm are two-fold:

- Mixed potential compression: The compression efficiencies of QR-based electric field integral

equation (EFIE) solvers depend on the methodology adopted to compress the scalar and vector potentials.

- Hierarchical form: The multilevel oct-tree structure (common to fast multipole approaches) and the QR compression efficiency are combined and further optimizations in the form of the merged interaction list (MIL) ensure a good overall performance.

A. Mixed Potential Scheme:

The key idea behind the compression is that the interaction sub-matrix between groups of well-separated basis-functions is low-ranked with a given tolerance level. If N_e^s and N_e^o are the number of edges in the well-separated source and the observer groups respectively and N_p^s and N_p^o are the corresponding number of patches, then the EFIE interaction sub-matrix is given by $\bar{\mathbf{Z}}_{N_e^o \times N_e^s}^{sub}$, which can be further represented into its components as:

$$\bar{\mathbf{Z}}_{N_e^o \times N_e^s}^{sub} = \bar{\mathbf{L}}_{N_e^o \times N_e^s}^{++} + \bar{\mathbf{L}}_{N_e^o \times N_e^s}^{--} + \bar{\mathbf{L}}_{N_e^o \times N_e^s}^{+-} + \bar{\mathbf{L}}_{N_e^o \times N_e^s}^{-+} + \bar{\mathbf{P}}_{N_e^o \times N_e^s}^{++} + \bar{\mathbf{P}}_{N_e^o \times N_e^s}^{--} + \bar{\mathbf{P}}_{N_e^o \times N_e^s}^{+-} + \bar{\mathbf{P}}_{N_e^o \times N_e^s}^{-+} \quad (8a)$$

where the component entries are given as in:

$$\bar{\mathbf{L}}_{ij}^{+-} = \frac{j\omega\mu}{4\pi} \int_{T_i^+} \int_{T_j^-} \frac{e^{-jk|\mathbf{r}-\mathbf{r}'|} \mathbf{f}_j^{T_j^-}(\mathbf{r}')}{|\mathbf{r}-\mathbf{r}'|} ds' \cdot \mathbf{f}_i^{T_i^+}(\mathbf{r}) ds \quad i=1,2,\dots,N_e^o; j=1,2,\dots,N_e^s \quad (8b)$$

and

$$\bar{\mathbf{P}}_{ij}^{+-} = \frac{1}{4j\omega\pi\epsilon} \int_{T_i^+} \int_{T_j^-} \frac{e^{-jk|\mathbf{r}-\mathbf{r}'|} \nabla' \cdot \mathbf{f}_j^{T_j^-}(\mathbf{r}')}{|\mathbf{r}-\mathbf{r}'|} ds' \nabla \cdot \mathbf{f}_i^{T_i^+}(\mathbf{r}) ds \quad i=1,2,\dots,N_e^o; j=1,2,\dots,N_e^s \quad (8c)$$

where $\mathbf{f}_j^{T_j^{+-}}$ denotes the half RWG [1] function $\mathbf{f}_j^{T_j^{+-}}$ which is defined on the positive or negative triangle as indicated in the superscript.

In PILOT compression is performed on the component sub-matrices. $\bar{\mathbf{Z}}_{N_e^o \times N_e^s}^{sub}$ is represented as:

$$\bar{\mathbf{Z}}_{N_e^o \times N_e^s}^{sub} = \bar{\mathbf{L}}_{N_e^o \times N_e^s} + \bar{\mathbf{B}}_{N_e^o \times N_p^o} \bar{\mathbf{P}}_{N_p^o \times N_p^s} \bar{\mathbf{B}}_{N_p^s \times N_e^s}^T \quad (9a)$$

where

$$\bar{\mathbf{L}}_{N_e^o \times N_e^s} = \bar{\mathbf{L}}_{N_e^o \times N_e^s}^{++} + \bar{\mathbf{L}}_{N_e^o \times N_e^s}^{--} + \bar{\mathbf{L}}_{N_e^o \times N_e^s}^{+-} + \bar{\mathbf{L}}_{N_e^o \times N_e^s}^{-+} \quad (9b)$$

$$\bar{\mathbf{B}}_{ij} = \begin{cases} 1 & \text{Patch } j \text{ is the positive patch of Edge } i \\ -1 & \text{Patch } j \text{ is the negative patch of Edge } i \\ 0 & \text{Patch } j \text{ does not belong to Edge } i \end{cases} \quad i=1,2,\dots,N_e^o; j=1,2,\dots,N_p \quad (9c)$$

$$\bar{\mathbf{P}}_{ij} = \frac{1}{4j\omega\pi\epsilon a_i a_j} \int_{T_i^+} \int_{T_j^-} \frac{e^{-jk|\mathbf{r}-\mathbf{r}'|}}{|\mathbf{r}-\mathbf{r}'|} ds' ds \quad i=1,2,\dots,N_p^o; j=1,2,\dots,N_p^s \quad (9d)$$

where a_i and a_j are the areas of the observer and source triangles respectively. The pre- and post-multiplier $\bar{\mathbf{B}}$ matrices are inherently sparse while the edge-by-edge $\bar{\mathbf{L}}$ matrix and the patch-by-patch $\bar{\mathbf{P}}$ matrix are compressed by applying QR decomposition on their sub-blocks $\bar{\mathbf{M}}_{m \times n}$ representing the corresponding interactions between well-separated m source basis functions and n observer basis functions:

$$\bar{\mathbf{M}}_{m \times n} = \bar{\mathbf{Q}}_{m \times r} \bar{\mathbf{R}}_{r \times n} \quad (10)$$

where r is the rank of $\bar{\mathbf{M}}_{m \times n}$ under the given tolerance \mathcal{E} and will henceforth be referred to as epsilon-rank.

B. Hierarchical Pre-Determined Matrix-Block Structure:

The oct-tree hierarchy common to multilevel fast multipole approaches is adopted. It is possible to compress each sub-matrix pertaining to the interaction between the observer basis functions residing in any cube and source basis functions residing in cubes within its interaction region. However, closer inspection reveals a pattern in the interaction shell of siblings that can be exploited to achieve further compression. It is possible to group source sibling cubes and common interaction region observer cubes in a merged interaction, in order to compress larger matrices to low epsilon-ranks and thereby gain in terms of overall compressibility. On further investigation it is observed that such a merged interaction may correspond to any one of the merged interaction patterns as shown in Fig. 3. The cubes in the middle are combination of observer siblings from the same sibling set and the darker cubes constitute the merged common interaction source region.

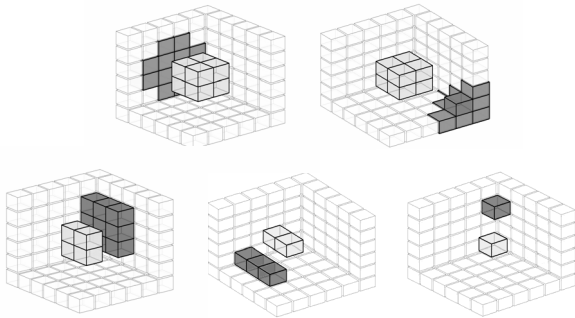


Figure 3. The types of merged interactions constituting the MIL

C Frequency Analysis

The QR-based algorithms degrade in compression efficiency as the structure size becomes much larger compared to the wavelength. More specifically, for significant compression efficiency, the variation in the kernel should be primarily due to the $\frac{1}{|\mathbf{r} - \mathbf{r}'|}$ decay rather than the $e^{-jk|\mathbf{r} - \mathbf{r}'|}$ oscillation. If in a given interaction the source and observer groups are much

larger compared to the wavelength, the rank of such an interaction matrix increases. The degradation of overall performance is demonstrated for a Hughes test chip in Fig. 4. The structure is discretized using 191390 unknowns and the memory requirement is plotted as a function of the electrical dimension of the structure.

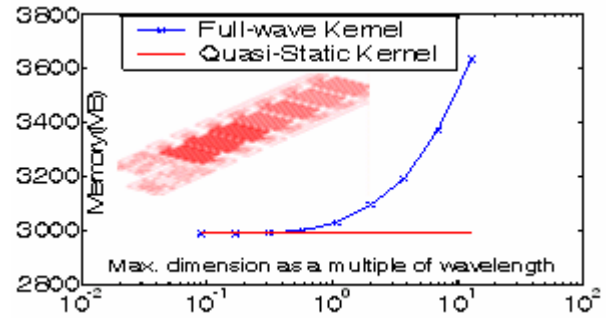


Figure 4. Memory required by the fast QR solver as a function of frequency

The memory requirement of the uncompressed matrix for the structure (Fig. 9) is 540GB. Hence, in spite of the apparent gradual degradation in performance, the algorithm is still a viable method of compression for structures with dimensions of multiple wavelengths. For structures described by complex surface meshes involving multiple length scales, such as those encountered in adaptive mesh refinement, the “electrically small” instability of classical FMMs may be exhibited for some interactions even if the overall structure is not electrically small. Therefore, for such problems, PILOT is a preferable alternative that will obviate any low-frequency instability.

IV NUMERICAL RESULTS

The coupled time domain EM/Circuit solver can be used for high speed interconnect and package modeling, signal integrity and EMI/EMC problems. The first numerical example in Fig. 5 shown here is the study on one of the ACES IEEE/EMC Society TC9 problems. The task was to investigate the non-ideal return path effect on high speed differential signaling. These results in Fig. 6 were consistent with the observations from other modeling methods [5]

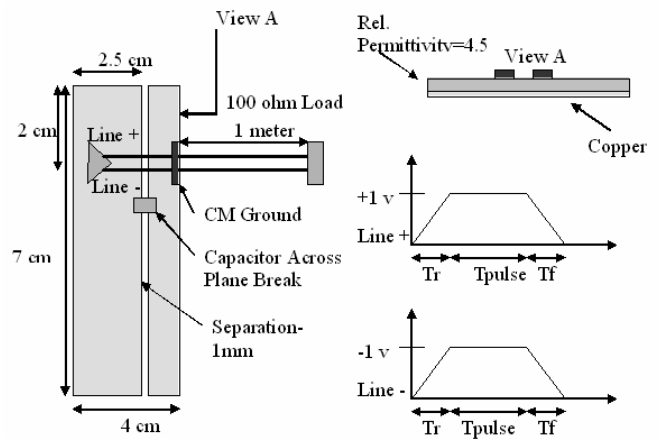


Figure 5. Differential pair over split plane and differential signal

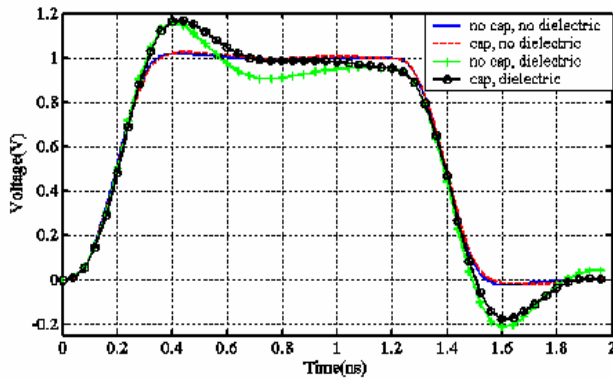


Figure 6. Voltage between Line+ and CM Ground point

The next example is a frequency domain coupled circuit-electromagnetic simulation of a LC matching network. Fig. 7 shows the surface current distribution for two different frequencies. At lower frequency the inductive portion of the structure has lower impedance and at higher frequency the capacitive part exhibits lower impedance, thereby altering the current flow and distribution.

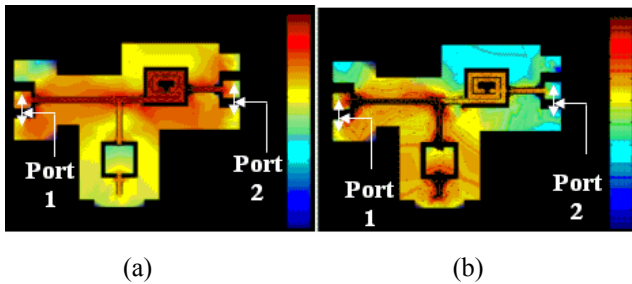


Figure 7. Surface current distribution on the LC tank layout, due to circuit excitation at port 1 at (a) 1 GHz (b) 20 GHz

Simulated magnitude and phase of the S parameters have been compared against measurement data in Fig. 8. In the coupled simulation, multiple vias in the original layout have been replaced with lumped circuit models to get a large reduction in the number of EM unknowns.

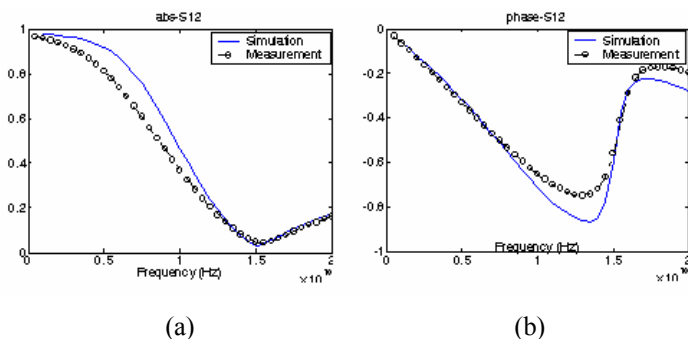


Figure 8. Correlation between the measurement and the simulation values of the frequency dependent scattering parameters (a) Magnitude (dB) (b) Phase (radians) for the structure shown in Fig. 7.

The accelerated version of the coupled solver is applied to a test chip (Fig. 9) containing meander lines, coplanar waveguides, capacitors and inductors at 3GHz. The time and

memory requirement for different discretization levels is plotted. It can be observed that the proposed multi-level QR-based solution technique scales linearly in both time and memory as we increase the number of unknowns.

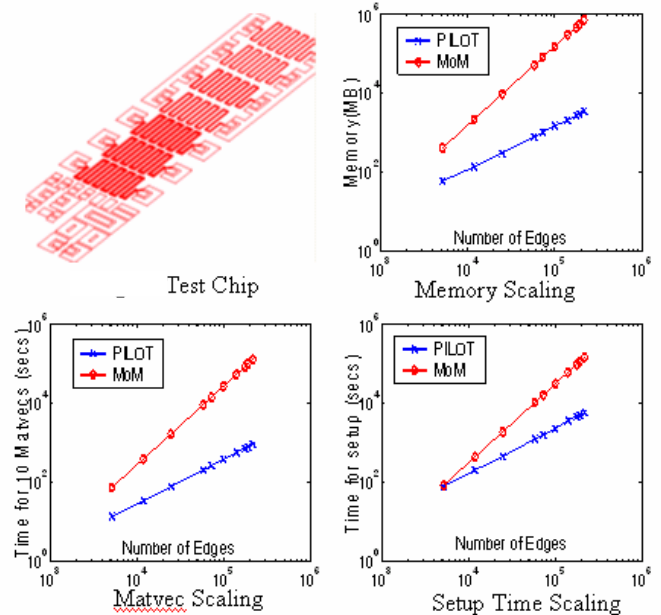


Figure 9. Test chip structure. Comparison of memory, set-up time and matrix vector product time between the proposed QR-based method (PILOT) and a brute force method.

REFERENCES

- [1] K. Aygun, B. Shanker, A. A. Ergin and E. Michielssen, "A two-level plane wave time-domain algorithm for fast analysis of EMC/EMI problems," *IEEE Trans. on Electromagnetic Compatibility*, vol 44, pp. 152-164, 2002
- [2] Yong Wang, Dipanjan Gope, Vikram Jandhyala and C.J. Richard Shi, "Generalized KVL-KCL Formulation for Coupled Electromagnetic-Circuit Simulation with Surface Integral Equations", *IEEE Trans. on Microwave Theory Tech.*, vol. 52, pp. 1673-1682, 2004.
- [3] D. H. Schaubert, D. R. Wilton, and A. W. Glisson, "A tetrahedral modeling method for electro-magnetic scattering by arbitrary shaped inhomogeneous dielectric bodies," *IEEE Trans. on Antennas and Propagation.*, vol. 32, pp. 77-85, 1984.
- [4] Dipanjan Gope and Vikram Jandhyala, "Oct-Tree Based Multilevel Low-Rank Decomposition Algorithm for Rapid 3D Parasitic Extraction", *IEEE Trans. on Computer-Aided Design of Integrated Circuits and Systems*, vol 23, pp 1673-1682, 2004.
- [5] A. E. Ruehli, "Equivalent circuit models for three dimensional multiconductor systems," *IEEE Trans. on Microwave Theory Tech.*, vol. 22, pp. 216-221, 1974.